

THE 2004 ULTRASONIC BENCHMARK PROBLEM - SDH RESPONSE UNDER OBLIQUE INCIDENCE: MEASUREMENTS AND PATCH ELEMENT MODEL CALCULATIONS

C.V. Krishnamurthy, M. Shankar, J.Vishnu Vardhan and Krishnan Balasubramaniam¹

Centre for NonDestructive Evaluation, ¹Department of Mechanical Engineering,
Indian Institute of Technology, Chennai, India 600 036

ABSTRACT. The 2004 ultrasonic benchmark problem requires models to predict, given a reference pulse waveform, the pulse echo response of cylindrical voids of various radii located in an elastic solid for various incidence angles of a transducer immersed in water. We present the results of calculations based on the patch element model, recently developed at CNDE, to determine the response of an SDH in aluminum for specific oblique incidence angles. Patch element model calculations for a scan across the SDH, involving a range of oblique incidence angles, are also presented. Measured pulse-echo scans involving the SDH response under oblique incidence conditions are reported. In addition, through transmission measurements involving a pinducer as a receiver and an immersion planar probe as a transmitter under oblique incidence conditions are also reported in a defect-free Aluminum block. These pinducer-based measurements on a defect-free block are utilised to characterize the fields at the chosen depth. Comparisons are made between predictions and measurements for the pulse-echo response of a SDH.

Keywords: ultrasonic transducer fields, beam model, scattering, benchmark, World Federation of NDE Centers

PACS: 43.20 Rz, 43.35 Cg, 43.35 Zc

INTRODUCTION

The World Federation of NDE Centres (WFNDEC), has defined benchmark problem sets [1] to encourage research communities across the world to compare and contrast different modeling approaches to evaluate pulse-echo responses from canonical flaws. The various contributions to the benchmark problems along with status reports are being published in the proceedings of the Review of the Quantitative Nondestructive Evaluation [2]. The responses from isolated flaws such as the flat-bottom-holes (FBH), side-drilled holes (SDH), spherical pores and cracks are required to be evaluated and compared with measurements posted at the website maintained by the WFNDEC [1].

Modeling these responses involves the determination of pressure/displacement fields in single media and across fluid-elastic solid interfaces, evaluation of flaw scattering characteristics and computing the pulse-echo responses. Many approximate schemes based on asymptotic techniques and numerical methods have been developed to deal with canonical problems [3 – 6]. Computational codes and simulation tools have also been implemented for laboratory use and for use by the industry [7,8]. Working on the benchmark problems offers modeling communities to rationalize various approaches and to present a clear picture on the status of the various schemes that can be utilized by the NDE community.

PATCH MODEL FOR THE PLANAR TRANSDUCER

The patch model is a conceptually simple scheme to evaluate the transducer fields in a homogenous medium at a single frequency [9]. It is understood that the RF waveforms in a pulsed experiment are to be obtained from many single frequency calculations and applying FFT routines. The model regards the transducer as made up of rectangular patch elements and invokes the superposition principle to evaluate the total transducer field from individual patch element fields. Figure 1 depicts the schematic of the patch model.

The key feature of the model is that the patch element dimensions are chosen such that the field point is in the far-field of the element. Since the far-field radiation pattern of a rectangular aperture is well-known and analytically expressible, the task of evaluating the complete transducer field is computationally simple. Consequently, as the field point moves farther from the transducer, the element dimensions increase and the number of elements eventually reduce to one as is to be expected. The total field from the transducer can be expressed as

$$p_0 = \frac{i\rho c\Delta A}{\lambda} \sum_{n=1}^N \frac{u_n}{R} e^{(-\alpha+ik)R} \text{sinc} \frac{k(x_n - x)\Delta w}{2R} \text{sinc} \frac{k(y_n - y)\Delta h}{2R} \quad (1)$$

where we have used the notation $\text{sinc} A = \frac{\sin A}{A}$. The elemental dimensions, Δw and Δh are chosen such that $z \gg (\Delta w)^2 / 4\lambda$ and $z \gg (\Delta h)^2 / 4\lambda$. In practice, a number F is chosen such that the following condition is ensured:

$$\Delta w \leq \sqrt{\frac{4\lambda z}{F}} \quad (2)$$

A similar procedure is adopted for Δh . Fields from a planar circular transducer in a single homogeneous medium have been computed using the patch model and verified through implementation of two alternate methods of evaluating the transducer fields [7,10] numerically both in the near-field and in the far-field.

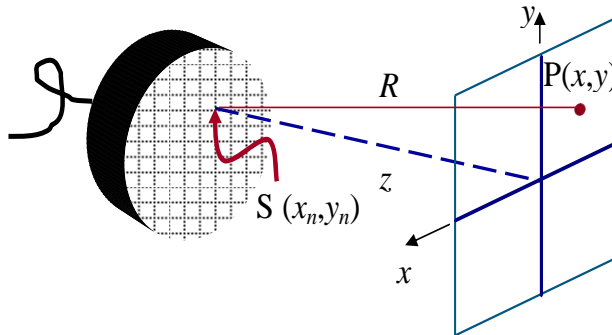


FIGURE 1. Schematic of the Patch Model for a Planar Transducer. The field at P is a superposition of the far-field contributions from all the patches. The far-field radiation pattern from each patch such as S is well-known.

The model as presented here has been extended in a straightforward manner to evaluate fields across planar interfaces between two media. To evaluate the transducer field across a planar interface, the dominant term of the solution for the field in the second medium from a point source located in the first medium. This dominant term, obtained through the method of steepest descent, represents the ray-based solution to the problem [11]. In the present context, the ray-based solution is taken to represent the fields from an effective point source – namely, the patch element as depicted in Figure 2.

Accordingly, the directivity D of the effective point source, defined in terms of the *sinc* functions, appears leading to the following expression for the displacement u in an elastic solid medium due to the source in a fluid medium

$$u(x, \omega) = \frac{-i\rho_1 v_o}{\rho_2 c_2} \frac{T_{12}(\theta_f) \exp(ik_1 s_1 + ik_2 s_2)}{\sqrt{\left(s_1 + \frac{s_2}{n}\right)} \sqrt{\left(s_1 + \frac{\cos^2(\theta_f)}{n \cos^2(\theta_s)} s_2\right)}} D \cdot dA. \quad (3)$$

The expression involves the plane wave transmission coefficient T_{12} , the densities of the two media (ρ_1, ρ_2), the appropriate velocity c_2 in medium 2, the phase factors and the slant path lengths s_1, s_2 . The particle velocity on the transducer, assumed to be constant over the entire face of the transducer, is denoted by v_o and the area of the elemental patch is denoted by dA . Using the superposition principle, the total transducer field in the second medium is evaluated from the individual patch element contributions. Figure 3 depicts displacement fields computed, by setting $v_o = 1$, for normal and oblique incidence angles for the benchmark configuration where the water path is 2" and the field plane is 1" below the water-aluminum interface [12]. The oblique incidence case includes longitudinal refraction angles of 30°, 45°, 60° and 70°.

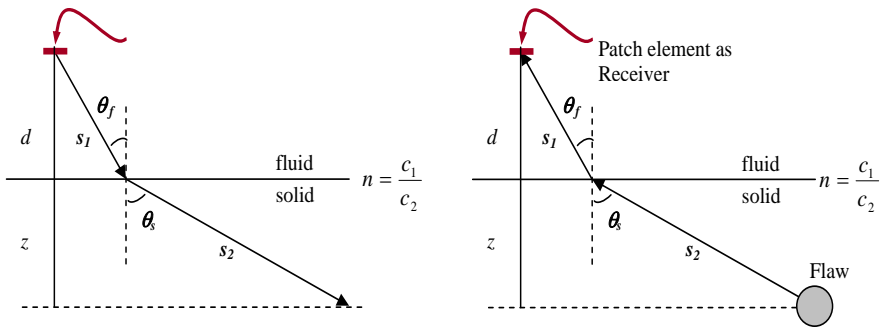


FIGURE 2. Each individual patch element simulates transmission and reception of ultrasound and is associated with a directivity D (Sinc functions). Flaw scattering is regarded as a secondary source radiation. Transmission and reception is modeled using rays following the method of steepest descent.

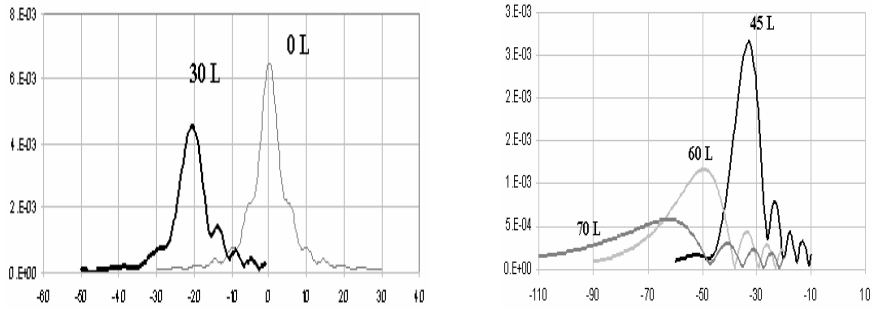


FIGURE 3. Computed longitudinal displacement fields for normal and oblique incidence angles across a water-aluminum interface. Peak lowering, peak shifting, and peak broadening as the refraction angle increases are features to note.

PINDUCER-BASED MEASUREMENTS

Measurements of the displacement field across the water-aluminum interface were carried out using a wideband pinducer for normal incidence and a few oblique incidence angles. Figure 4 shows the results.

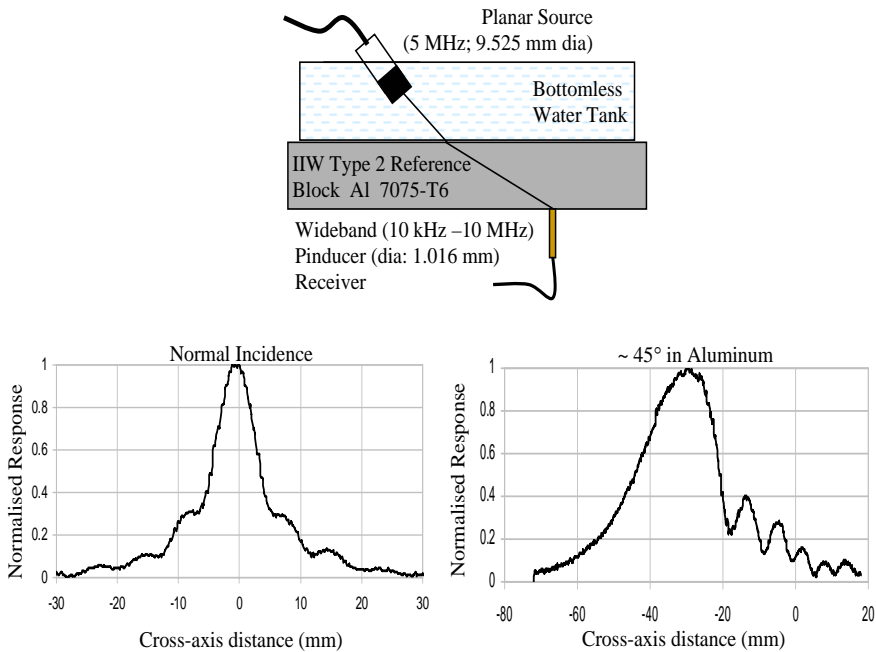


FIGURE 4. The schematic for the pinducer-based measurement is shown in the top panel. The single frequency component of the measured pinducer signal is shown in the lower panels as a function of the relative positions between the transmitter and the receiver for normal and oblique incidence. A 0.1 mm scan step was used in all these measurements. The broad maximum at higher refracted angles made extraction of single frequency component difficult from measurements.

PULSE-ECHO RESPONSE FROM SDH

The patch element model was used to evaluate the pulse-echo response from canonical flaws such as the SDH. The signal reception process involves the evaluation of the pressure generated by the flaw and averaged over the receiver area. The formal expression utilised in the present context is given below:

$$P_{avg}^{p:p}(\omega) = \frac{i\omega\rho_2c_{p2}U_{inc}(\omega)}{S_r} \int_{S_r} \frac{A^{p:p}(\omega)T_{21}^{p:p}(\theta_s) \exp[i(k_{p1}s_1 + k_{p2}s_2)]}{\sqrt{s_2 + \frac{c_{p1}}{c_{p2}}s_1} \sqrt{s_2 + \frac{n \cos^2 \theta_s}{\cos^2 \theta_f} s_1}} dS \quad (4)$$

The above expression involves the displacement field incident on the flaw, the flaw scattering cross-section, and all the factors corresponding to rays transmitted from the flaw across the interface to the receiver. It can be seen that the flaw response and the beam profile combine to determine the echo signal characteristics. To validate the transducer beam features, a side drilled hole (SDH) of a small diameter was chosen to keep flaw scattering simple in the angular domain. Figure 5 shows SDH echo signal peak positions as well as the echo signal profile as a function of position from SDH measured on a beam profile block.

The measurements were repeated using a contact transducer. Figure 6 shows the results of the pulse-echo peak positions obtained with both P-waves and SV-waves.

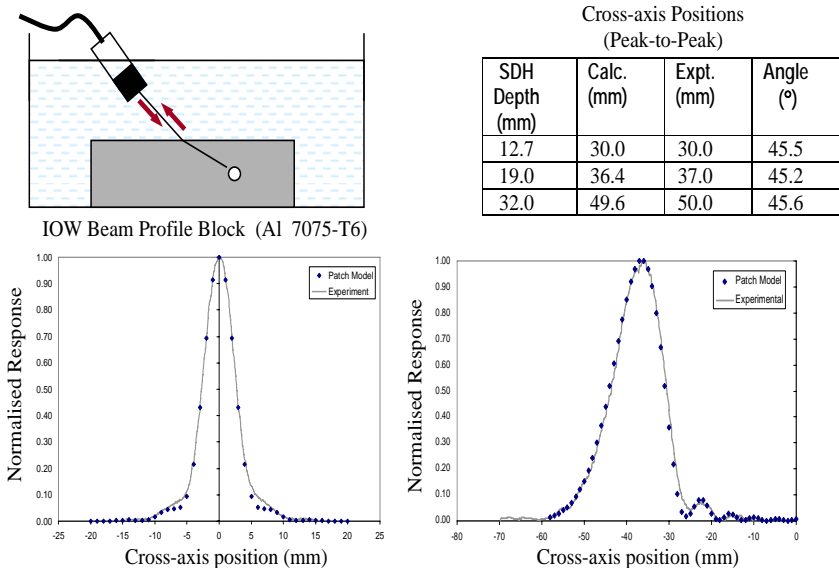
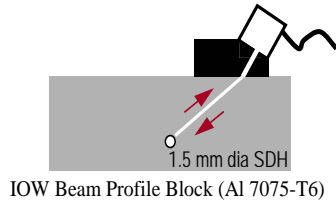


FIGURE 5. The schematic for the pulse echo measurements on a standard IOW beam profile block is shown in the top left panel. The Table on the top right panel indicates the pulse-echo peak positions for various SDH depths. The refracted angle at these depths is nearly constant as is to be expected. The lower panels show a comparison between computed and measured single frequency (5 MHz) response of the pulse-echo signals at normal and oblique incidence. The agreement between model and experiment can be seen to be very good.

Cross-axis Positions (Peak-to-Peak)

P-wave Refracted Angle (°)	Incident Field Peak Position Calc. (mm)	Measured Pulse-Echo Peak Position (mm)
49.5	22.4	23.5
55.4	26.0	26.3
61.7	28.8	30.6



Cross-axis Positions (Peak-to-Peak)

SDH Depth (mm)	30° SV		45° SV		60° SV	
	Expt. (mm)	Calc. (mm)	Expt. (mm)	Calc. (mm)	Expt. (mm)	Calc. (mm)
12.7	9.0	7.7	13.0	12.5	23.0	21.4
19.0	13.0	12.4	20.5	19.1	34.0	31.9
32.0	22.5	21.4	32.5	31.7	53.5	53.6
50.0	37.5	32.2	52.0	49.8	86.5	84.5

FIGURE 6. The top panel shows the schematic of the contact transducer (0.25” dia) measurement of pulse echo signals from SDH flaws in a standard IOW beam profile block. At 5 MHz, the peaks of the single frequency beam profile are compared with incident field maxima evaluated using the patch model. The slant path in Plexiglas is 9 mm.

While the predictions agree with measurements in general, the discrepancy between incident field maxima and the pulse-echo maxima at large refracted angles can be understood to be due to the systematic modification of the pulse-echo response by the SDH at these high refracted angles. As the flaw (SDH) size (dia) increases, the flaw scattering characteristics are expected to modify the pulse-echo response significantly. In particular, for a larger SDH, the discrepancy noted above is expected to increase.

THE 2004 BENCHMARK PROBLEM – SDH RESPONSE

The 2004 benchmark problem involves the prediction and validation of the pulse-echo response from a 4 mm dia SDH located at a 1.0” depth in Aluminum for normal incidence, oblique P-wave and SV-wave incidence angles. Figure 7 shows the results obtained using the patch element model and the separation of variables method [13] of evaluating the SDH response.

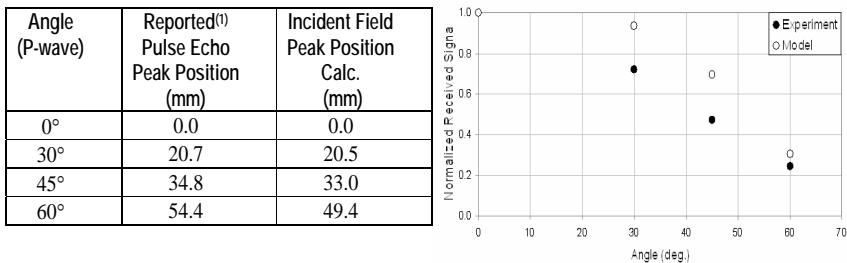


FIGURE 7. The Table on the left compares the reported measurements of the pulse-echo peak positions with computed incident field peak positions for various P-wave refracted angles. On the right, the model predictions for the magnitude of the pulse echo response is compared with reported measurements.

The higher discrepancy between the incident field peak position and the corresponding pulse-echo peak position for the 60° P-wave case is, we believe, due to the larger size of the SDH. While the trends in the predicted pulse-echo amplitude compare well with the reported measurements, a more detailed calculation taking into account incident field variations seems necessary.

THE 2005 BENCHMARK PROBLEM – CRACK RESPONSE

The 2005 benchmark problem deals with prediction and validation of pulse-echo response from tight cracks in an attenuating medium, namely, a Titanium alloy. Figure 8 shows the results obtained using the patch element model. The calculations were carried out over a frequency band, taking into account frequency-dependent attenuation of Titanium, to obtain the pulse-echo responses for the two cracks.

From Figure 8 it appears that model predictions underestimate the magnitude of the pulse-echo response. However, since the model has been verified and validated with DGS curves published earlier, it is believed that there could be errors in pulse-echo measurements and/or in attenuation estimates provided for the calculation.

SUMMARY

An explicit transducer field evaluator - the patch element model – introduced last year has been used to evaluate the responses from a SDH and two tight cracks which are part of the 2004 and 2005 Benchmark Problems defined by WFNDEC. This model has been used to compute pressure/displacement fields under normal and oblique incidence angles in single media as well as across water-aluminum interfaces. Pinducer-based measurements

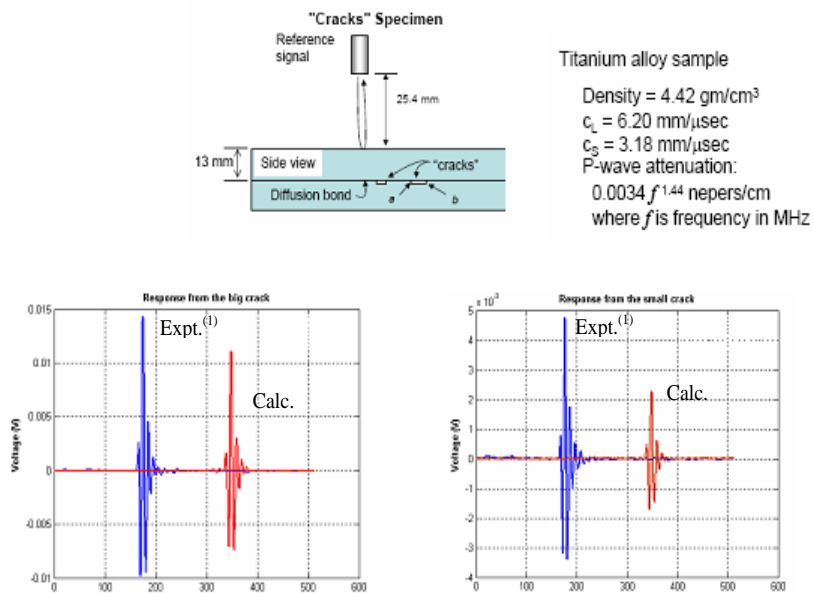


FIGURE 8. The schematic of the 2005 benchmark problem dealing with tight cracks in Titanium alloy is shown in the top panel. The bottom panel shows the computed pulse-echo responses at normal incidence for the two cracks with the reported measurements. The pulse echo signals are shown displaced for clarity.

were carried out to determine the displacement fields across the water-aluminum interface. Further, pulse-echo measurements were carried out on an IOW Beam Profile Block having 1.5 mm dia SDHs at various depths. These measurements were used to validate the trends predicted by the Patch element model. The response of a 4 mm dia SDH defined by WFNDEC was evaluated in the frequency domain and compared with reported measurements. The agreement has been found to be reasonable. The pulse-echo response from two tight cracks in Titanium alloy was also computed, taking into account frequency-dependent attenuation, and compared with reported measurements. The agreement is reasonable. Work is in progress to account for the pulse-echo response under non-uniform insonification of SDHs and cracks.

REFERENCES

1. The website <http://www.wfndec.org> outlines the scope and details the benchmark problems in various fields of Nondestructive testing/evaluation.
2. R.B. Thompson, "An Ultrasonic Benchmark Problem: Overview and Discussion of Results", in *Review of Progress in Nondestructive Evaluation*, **21B**, edited by D. O. Thompson and D. E. Chimenti, AIP, Melville, NY, 2001, pp 1917-1924.
3. C.V. Krishnamurthy., M. Shankar and Krishnan Balasubramaniam, "Ultrasonic Benchmark Problem 2002: Measurements and Numerical Experiments", in *Review of Quantitative Nondestructive Evaluation*, vol. **23**, 1545-1552 (2004)
4. N. Gengembre and A. Lhémy, "Pencil Method in Elastodynamics: Application to Ultrasonic Field Computation", *Ultrasonics*, vol. **38**, 495-499 (2000)
5. D. Gridin, and L.J. Fradkin, "High-frequency Asymptotic Description of Pulses Radiated by a Circular Normal Transducer into an Elastic Half-space", *Journal of Acoustical Society of America*, vol. **104**(6), 3190-3198 (1998).
6. T.P. Lerch., L.W. Schmerr and A. Sedov, "Modeling the Ultrasonic Radiation of a Planar Transducer through a Plane Fluid-Solid Interface", *Research in Nondestructive Evaluation*, vol.**11**, 137-163 (1999).
7. L.W.Schmerr, *Fundamentals of Ultrasonic Non-destructive Evaluation – A Modeling Approach*, Plenum, NY, 1998.
8. P. Calmon, A. Lhémy, I. Lecœur-Taïbi, and R. Raillon, "Recent Developments in Ultrasonic NDT Modelling", in *CIVA, 15th World Conference on Non-Destructive Testing* 15-21 October 2000, Rome.
9. K.B. Ocheltree and L.A. Frizzell, "Sound Field Calculation for Rectangular Sources", *IEEE Trans UFFC*, vol.**36**, 242-248, (1989).
10. G.S. Kino, *Acoustic Waves – Devices, Imaging, and Analog Signal Processing*, Prentice-Hall, NJ, (1987), pp 164-175.
11. L.M. Brekhovskikh, *Waves in Layered Media*, Academic Press (1960) pp 292-324.
12. Krishnamurthy C.V., Shankar M. and Krishnan Balasubramaniam, "Patch Element Model for the Evaluation of Displacement Fields within an Elastic Solid from a Non-Contact Immersion Transducer: Application to the 2004 Ultrasonic Benchmark Problem", in *Review of Quantitative Nondestructive Evaluation*, vol. **24B**, edited by D. O. Thompson and D. E. Chimenti, AIP, Melville, NY, 2005, pp. 1864-1871.
13. Y.H. Pao and C.C. Mow, *Diffraction of Elastic Waves and Dynamic Stress Concentrations*, The Rand Corporation, 1973.